

Decay law of magnetic turbulence with helicity balanced by chiral fermions

Axel Brandenburg ^{1,2,3,4}, Kohei Kamada ⁵, and Jennifer Schober ⁶¹*Nordita, KTH Royal Institute of Technology and Stockholm University, 10691 Stockholm, Sweden*²*The Oskar Klein Centre, Department of Astronomy, Stockholm University, AlbaNova, 10691 Stockholm, Sweden*³*School of Natural Sciences and Medicine, Ilia State University, 0194 Tbilisi, Georgia*⁴*McWilliams Center for Cosmology and Department of Physics, Carnegie Mellon University, Pittsburgh, Pennsylvania 15213, USA*⁵*Research Center for the Early Universe (RESCEU), Graduate School of Science,**The University of Tokyo, Hongo 7-3-1, Bunkyo-ku, Tokyo 113-0033, Japan*⁶*Institute of Physics, Laboratory of Astrophysics, École Polytechnique Fédérale de Lausanne (EPFL), 1290 Sauverny, Switzerland*

(Received 1 February 2023; accepted 4 April 2023; published 11 May 2023)

In plasmas composed of massless electrically charged fermions, chirality can be interchanged with magnetic helicity while preserving the total chirality through the quantum chiral anomaly. The decay of turbulent energy in plasmas such as those in the early Universe and compact stars is usually controlled by certain conservation laws. In the case of zero total chirality, when the magnetic helicity density balances with the appropriately scaled chiral chemical potential to zero, the total chirality no longer determines the decay. We propose that in such a case, an adaptation to the Hosking integral, which is conserved in nonhelical magnetically dominated turbulence, controls the decay in turbulence with helicity balanced by chiral fermions. We show, using a high resolution numerical simulation, that this is indeed the case. The magnetic energy density decays and the correlation length increases with time just like in nonhelical turbulence with vanishing chiral chemical potential. But here, the magnetic helicity density is nearly maximum and shows a scaling with time t proportional to $t^{-2/3}$. This is unrelated to the $t^{-2/3}$ decay of magnetic energy in fully helical magnetic turbulence. The modulus of the chiral chemical potential decays in the same fashion. This is much slower than the exponential decay previously expected in theories of asymmetric baryon production from the hypermagnetic helicity decay after axion inflation.

DOI: [10.1103/PhysRevResearch.5.L022028](https://doi.org/10.1103/PhysRevResearch.5.L022028)

Magnetic helicity characterizes the knottedness of magnetic field lines and plays important roles in cosmological, astrophysical, and laboratory plasmas. Since the early work of Woltjer in 1958 [1], we know that the magnetic helicity is an invariant of the ideal magnetohydrodynamic (MHD) equations. Even in the nonideal case of finite conductivity, it is asymptotically conserved in the limit of large magnetic Reynolds numbers [2]. This is because, unlike the magnetic energy dissipation, which is finite at large magnetic Reynolds numbers, the magnetic helicity dissipation converges to zero in that limit [3]. The magnetic helicity controls the decay of magnetic fields in closed or periodic domains, provided the magnetic helicity is finite. However, even when the net magnetic helicity over the whole volume vanishes, there can still be random fluctuations of magnetic helicity. In this case, the conservation of magnetic helicity still plays an important role, but only in smaller subvolumes, as was shown recently [4]. The conserved quantity in that case is what is now known as the Hosking integral [5,6], which characterizes magnetic helicity fluctuations in smaller subvolumes [4].

At relativistic energies, the chirality of fermions combines with the helicity of the magnetic field to a total chirality that

is *strictly* conserved in a periodic or closed domain—even for finite magnetic diffusivity [7,8] which is a consequence of the chiral anomaly [9,10]. This can have a number of consequences. There is an instability that can amplify a helical magnetic field [11]. It is now often referred to as the chiral plasma instability (CPI) [12] and it causes the chiral chemical potential carrying the chirality of the fermions to decay such that the total chirality remains unchanged [13–15]. Conversely, if a helical magnetic field decays, the chiral chemical potential can increase [16,17]. Finally, when the chiral chemical potential balances the magnetic helicity to produce vanishing total chirality of the system, which is realized in, e.g., cosmological MHD after axion inflation [18–20], the magnetic field can only decay. It has been thought that the decay is triggered by the CPI and that it would be therefore exponential [18,19]. In this Letter, however, we show that this decay occurs only in a power-law fashion. This has consequences for explaining the baryon asymmetry of the Universe [21–23] and for theories of primordial magnetic fields, which will open up a new direction for early Universe cosmology model building. The purpose here is to show that the decay of the magnetic field in chiral MHD is governed—similarly to nonhelical MHD—by a conserved quantity that we call the adapted Hosking integral. While the model adopted here is based on quantum electrodynamics, the extension to the realistic cosmological models based on the standard model of particle physics is straightforward; see, e.g., Refs. [14,24].

Published by the American Physical Society under the terms of the [Creative Commons Attribution 4.0 International license](https://creativecommons.org/licenses/by/4.0/). Further distribution of this work must maintain attribution to the author(s) and the published article's title, journal citation, and DOI. Funded by [Bibsam](https://www.bibsam.com/).

The Hosking integral I_H is defined as the asymptotic limit of the relevant magnetic helicity density correlation integral, $\mathcal{I}_H(R)$, for scales R which are large compared to the correlation length of the turbulence, ξ_M , but small compared to the system size L . The function $\mathcal{I}_H(R)$ is given by

$$\mathcal{I}_H(R) = \int_{V_R} \langle h(\mathbf{x})h(\mathbf{x} + \mathbf{r}) \rangle d^3r, \quad (1)$$

where V_R is the volume of a ball of radius R and, in MHD, $h = \mathbf{A} \cdot \mathbf{B}$ is the magnetic helicity density with \mathbf{A} being the magnetic vector potential, so $\mathbf{B} = \nabla \times \mathbf{A}$. Here, angle brackets denote averages over the volume L^3 .

For relativistic chiral plasmas, on the other hand, we now amend the magnetic helicity density with a contribution from the chiral chemical potential μ_5 . We work here with the scaled chiral chemical potential $\mu_5 \rightarrow \mu'_5 = (4\alpha/\hbar c)\mu_5$, where α is the fine structure constant, \hbar is the reduced Planck constant, and c is the speed of light. Our rescaled μ'_5 has the dimension of a wave number. From now on, we drop the prime and only work with the rescaled chiral chemical potential. We also define the quantity $\lambda = 3\hbar c (8\alpha/k_B T)^2$, where k_B is the Boltzmann constant and T is the temperature. We define the total helicity density $h_{\text{tot}} \equiv \mathbf{A} \cdot \mathbf{B} + 2\mu_5/\lambda$ and replace $h \rightarrow h_{\text{tot}}$ when defining the adapted Hosking integral.

Similarly to earlier studies of nonrelativistic chiral plasmas ($\mu_5 \rightarrow 0$) with a helical magnetic field, the case of a finite net chirality, $\langle h_{\text{tot}} \rangle \neq 0$, is governed by the conservation law for $\langle h_{\text{tot}} \rangle$. Of course, when $\langle h_{\text{tot}} \rangle = 0$, it is still conserved, but it can then no longer determine the dynamics of the system. This is when we expect, instead, I_H to control the dynamics of the decay. As before, we define $I_H = \mathcal{I}_H(R_*)$ for values of R_* for which $\mathcal{I}_H(R)$ shows a plateau. In the following, we focus on this case using numerical simulations to compute the decay properties of a turbulent magnetic field and the conservation properties of I_H using the total helicity in a relativistic plasma.

Now, setting $c = 1$, the evolution equations for \mathbf{A} and μ_5 are [8]

$$\frac{\partial \mathbf{A}}{\partial t} = \eta(\mu_5 \mathbf{B} - \mathbf{J}) + \mathbf{u} \times \mathbf{B}, \quad \mathbf{J} = \nabla \times \mathbf{B}, \quad (2)$$

$$\frac{\partial \mu_5}{\partial t} = -\frac{2}{\lambda} \eta(\mu_5 \mathbf{B} - \mathbf{J}) \cdot \mathbf{B} - \nabla \cdot (\mu_5 \mathbf{u}) + D_5 \nabla^2 \mu_5, \quad (3)$$

where η is the magnetic diffusivity, D_5 is the diffusion coefficient of μ_5 , spin flipping is neglected here, and \mathbf{u} is the velocity, which is governed by the compressible Navier-Stokes equations [8,25,26]

$$\frac{D\mathbf{u}}{Dt} = \frac{2}{\rho} \nabla \cdot (\rho \nu \mathbf{S}) - \frac{1}{4} \nabla \ln \rho + \frac{\mathbf{u}}{3} (\nabla \cdot \mathbf{u} + \mathbf{u} \cdot \nabla \ln \rho) - \frac{\mathbf{u}}{\rho} [\mathbf{u} \cdot (\mathbf{J} \times \mathbf{B}) + \eta \mathbf{J}^2] + \frac{3}{4\rho} \mathbf{J} \times \mathbf{B}, \quad (4)$$

$$\frac{\partial \ln \rho}{\partial t} = -\frac{4}{3} (\nabla \cdot \mathbf{u} + \mathbf{u} \cdot \nabla \ln \rho) + \frac{1}{\rho} [\mathbf{u} \cdot (\mathbf{J} \times \mathbf{B}) + \eta \mathbf{J}^2], \quad (5)$$

where $\mathbf{S}_{ij} = (\partial_i u_j + \partial_j u_i)/2 - \delta_{ij} \nabla \cdot \mathbf{u}/3$ are the components of the rate-of-strain tensor, ν is the kinematic viscosity, ρ is the density (which includes the rest mass density), and the

ultrarelativistic equation of state for the pressure $p = \rho/3$ has been employed. We assume uniform ν , η , and D_5 such that $\nu = \eta = D_5$. Our use of Eqs. (4) and (5) compared to the nonrelativistic counterpart only affects the kinetic energy and not the magnetic field evolution; see Ref. [27] for comparisons in another context.

We define spectra of a quantity $h(\mathbf{x})$ as $\text{Sp}(h) = \int_{4\pi} |\tilde{h}|^2 k^2 d\Omega_k / (2\pi L)^3$, where a tilde denotes the quantity in Fourier space and Ω_k is the solid angle in Fourier space, so that $\int \text{Sp}(h) dk = \langle h^2 \rangle$. Here, $k \equiv |\mathbf{k}|$. The magnetic energy spectrum is $E_M(k, t) \equiv \text{Sp}(\mathbf{B})/2$ and $\int E_M dk = \langle \mathbf{B}^2 \rangle/2$ is the mean magnetic energy density. The mean magnetic helicity density is $\mathcal{H}_M = \langle \mathbf{A} \cdot \mathbf{B} \rangle$, the magnetic helicity spectrum is $H_M(k, t)$ with $\int H_M dk = \mathcal{H}_M$, and $\xi_M = \mathcal{E}_M^{-1} \int k^{-1} E_M dk$ is the correlation length.

For an initially uniform $\mu_5 \equiv \mu_{50}$, Eq. (2) has exponentially growing solutions proportional to $e^{i\mathbf{k} \cdot \mathbf{x} + \gamma_5 t}$, when $k < \mu_{50}$. The maximum growth rate is $\gamma_5 = \mu_{50}^2 \eta/4$ for $k = k_5 \equiv \mu_{50}/2$ [8,25]. As an initial condition for \mathbf{A} , we consider a Gaussian distributed random field with a magnetic energy spectrum that is a broken power law with $E_M(k, t) \propto k^4$ for $k < k_0$, motivated by causality constraints [28], and a Kolmogorov-type spectrum, $E_M(k, t) \propto k^{-5/3}$, for $k > k_0$, which may be expected if there is a turbulent forward cascade. By setting $k_0 = 1$ for the spectral peak, we fix the units of velocity and length. The unit of time is then $(k_0)^{-1}$. We initially set $\rho = \rho_0 = 1$, which then also fixes the units of energy.

We solve the governing equations using the PENCIL CODE [29], where the equations are already implemented [30,31]. We consider a cubic domain of size L^3 , so the smallest wave number is $k_1 = 2\pi/L$. The largest wave number is $k_{N_y} = k_1 N/2$, where N is the number of mesh points in one direction. In choosing our parameters, it is important to observe that $k_1 \ll k_0 \ll k_5 \ll k_{N_y}$. Here, we choose $k_1 = 0.02$, $k_0 = 1$, $k_5 = 5$, and $k_{N_y} = 10.24$, using $N = 1024$ mesh points in each of the three directions. This means that $|\mu_{50}| = 10$, which is virtually the same as k_{N_y} . However, experiments with other choices, keeping $N = 1024$, showed that ours yields an acceptable compromise that still allows us to keep k_1 small enough. We choose the sign of μ_5 to be negative, and adjust the amplitude of the magnetic field such that $2\mathcal{E}_M \xi_M = \mathcal{H}_M = -2\mu_{50}/\lambda$. Using $\eta = 2 \times 10^{-4}$ and $\lambda = 2 \times 10^4$, we have, following Ref. [27], $v_\lambda \equiv \mu/\sqrt{\rho_0 \lambda} \approx 0.07$ and $v_\mu \equiv \mu\eta = 0.002$, so $v_\lambda/v_\mu \approx 35 \gg 1$, corresponding to what is called regime I.

In Fig. 1(a), we present magnetic energy spectra at different times. We clearly see an inverse cascade where the spectral magnetic energy increases with time for $k \ll k_0$ (indicated by the upward arrow), but decays for $k \gg k_0$. As time goes on, the peak of the spectrum moves to smaller wave numbers with $k_{\text{peak}} \approx \xi_M^{-1}$, where ξ_M increases approximately like a power law, $\xi_M \propto t^q$, while the energy density decreases, also approximately like a power law with $\mathcal{E}_M \propto t^{-p}$. The spectral peak always evolves underneath an envelope $\propto k^{3/2}$, which implies that $\max[E_M(k, t)] = \xi_M(t)^{-\beta}$ with $\beta = 3/2$, indicated by the upper dashed dotted line in Fig. 1(a).

To compute \mathcal{I}_H (and thereby I_H), we employ a spectral technique by computing the total helicity variance spectrum $\text{Sp}(h_{\text{tot}})$; see Fig. 1(b). Compared to the inverse cascade seen in $\text{Sp}(\mathbf{B})$, here we see the conservation of the large-scale total

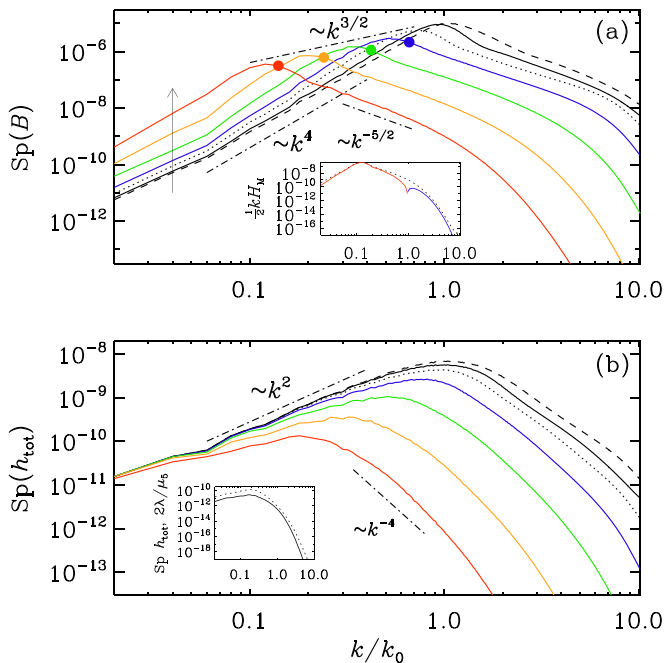


FIG. 1. (a) Magnetic energy and (b) total helicity variance spectra at $t = 31$ (dashed), 100 (solid), 316 (dotted), 10^3 (blue), 3.16×10^3 (green), 10^4 (orange), and 3.16×10^4 (red). In (a), note that $\text{Sp}(\mathbf{B})$ evolves underneath the envelope $k^{3/2}$, and the upward arrow indicates the sense of time. For orientation, the slopes $k^{-5/2}$ and k^{-4} have been indicated in what is expected to correspond to the inertial ranges in (a) and (b), respectively. In (a), the inset shows $(k/2)H_M(k)$ at the last time with positive (negative) values in red (blue), and in (b), the inset compares $\text{Sp}(2\mu_5/\lambda)$ (solid) with $\text{Sp}(h_{\text{tot}})$ (dotted) at the last time.

helicity variance spectrum $\propto k^2$. We thus obtain

$$\mathcal{I}_H(R, t) = L^{-3} \int w(\mathbf{k}, R) \text{Sp}(h_{\text{tot}}) d^3\mathbf{k} / (2\pi)^3. \quad (6)$$

We choose $w(\mathbf{k}, R) = (4\pi R^3/3)[6j_1(kR)/kR]^2$ as weight function [6] with j_n being spherical Bessel functions.

In Fig. 2, we plot the adapted Hosking integral $I_H(t)$, normalized by its initial value. It is evaluated as $I_H(t) = \mathcal{I}_H(R_*, t)$ with $k_0 R_* = 100$, where $\mathcal{I}_H(R, t)$ is shown in the inset at different times as functions of R . Note that $I_H(t)$ is essentially flat and shows only toward the end a slight decline $\propto t^{-0.12}$, which is similar to what has been seen for other simulations at that resolution; see, e.g., Ref. [32]. Thus, the adapted Hosking integral appears to be well conserved—even better so than the Hosking integral in ordinary MHD, studied in Refs. [4,6]. There is not even the slight uprise $I_H(t)$ reported in Ref. [6], which was there argued to be due to strong non-Gaussian contributions to the field that emerged during the nonlinear evolution of the system. Note also that for $R \ll R_*$, we see $\mathcal{I}_H(R, t) \propto R^2$, which is shallower than the expected cubic scaling. This might change at larger resolution, although an intermediate range $\propto R^2$ is also seen in Fig. 4(d) of Ref. [6], before cubic scaling emerged for $R/2\pi < 10^{-4}$.

As in the case of nonrelativistic MHD ($\mu_5 \rightarrow 0$), the dimensions of \mathcal{I}_H and I_H are $\text{cm}^3 \text{s}^{-4}$. This implies that in $\xi_M \propto t^q$, the value of the exponent is $q = 4/9$, if the conservation

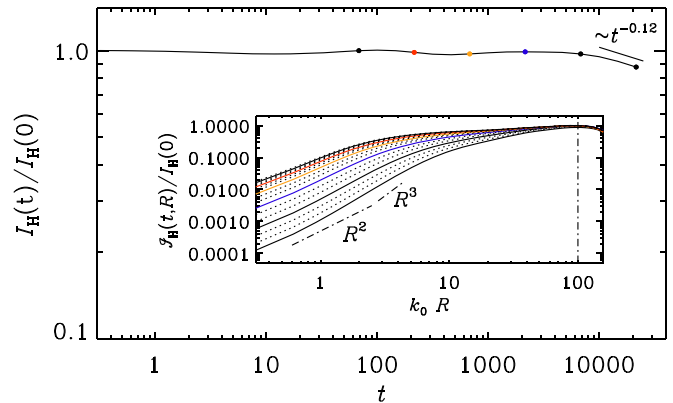


FIG. 2. $I_H(t)$ normalized by its initial value. The inset shows $\mathcal{I}_H(R, t)$ versus R at different times t : solid lines correspond to $t = 70, 200, 700, 2000, 7000$, and 20000 , which are also marked by selected colored symbols in the graph of $I_H(t)$. The adapted Hosking integral is evaluated as $I_H(t) = \mathcal{I}_H(R_*, t)$. The vertical dashed-dotted line marks the value $k_0 R_* = 100$ where the curves show a plateau. The slopes $\propto R^2$ and $\propto R^3$ are also marked by dashed-dotted lines.

of \mathcal{I}_H determines the time evolution of the magnetic field around the characteristic scale. Next, assuming self-similarity, the magnetic spectra can be collapsed on top of each other by plotting them versus $k\xi_M(t)$ and compensating the decline in the height by ξ_M^β to yield the universal function $\phi(k\xi_M) = \xi_M^\beta E_M(k\xi_M)$; see Appendix B of Ref. [6] and Refs. [32,33] for examples in other contexts. Using also the invariance of the spectrum under rescaling [34], $\mathbf{x} \rightarrow \mathbf{x}' = \mathbf{x}\ell$ and $t \rightarrow t' = t\ell^{1/q}$, and since the dimension of $E_M(k, t)$ is $\text{cm}^3 \text{s}^{-2}$, we have $E_M(k\ell^{-1}, t\ell^{1/q}) = \ell^{3-2/q+\beta}[\xi_M\ell]^{-\beta}\phi(k\xi_M)$, and therefore $\beta = 2/q - 3 = 3/2$, which agrees with Fig. 1(a). Finally, for $\mathcal{E}_M \propto t^{-p}$, we find with $\mathcal{E}_M(t) = \int E_M dk \propto t^{-(\beta+1)q}$ the line $p = 2(1 - q)$, which is also known as the self-similarity line [6,33]. With $q = 4/9$, we thus obtain $p = 10/9$. This is completely analogous to the MHD case with zero magnetic helicity [35]; see also Table 2 of Ref. [32]. Thus, the cancellation of finite magnetic helicity by fermion chirality with $\mathcal{H}_M(t) = -2\langle\mu_5\rangle(t)/\lambda \neq 0$ has the same effect as that of zero magnetic helicity.

To understand the decay of magnetic helicity density in the present simulations, it is important to remember that the real space realizability condition of magnetic helicity [36] is always valid and implies $|\mathcal{H}_M| \leq 2\mathcal{E}_M\xi_M$. Assuming the inequality to be saturated, we find the scaling $|\mathcal{H}_M| \propto |\langle\mu_5\rangle| \propto t^{-r}$ with $r = p - q = 2/3$. This is well obeyed, as is shown in Fig. 3. In the inset, we show that $2\mathcal{E}_M\xi_M/\mathcal{H}_M \approx 1$ at early times and about 1.1 at late times. It is thus fairly constant, therefore confirming the validity of our underlying assumption. On top of this evolution of the chiral asymmetry, the growth rate of the CPI, $\gamma_5 \propto \langle\mu_5\rangle^2 \propto t^{-4/3}$, decays more rapidly than t^{-1} , which causes it to grow less efficiently so as not to spoil the scaling properties of the system.

To characterize the scaling expected from the conservation of the adapted Hosking integral further, in Fig. 4 we plot the pq diagram of the instantaneous scaling exponents $p(t) = -d \ln \mathcal{E}_M / d \ln t$ versus $q(t) = d \ln \xi_M / d \ln t$. The solution converges to a point close to the crossing point between the $\beta = 3/2$ line and the scale-invariance line $p = 2(1 - q)$.

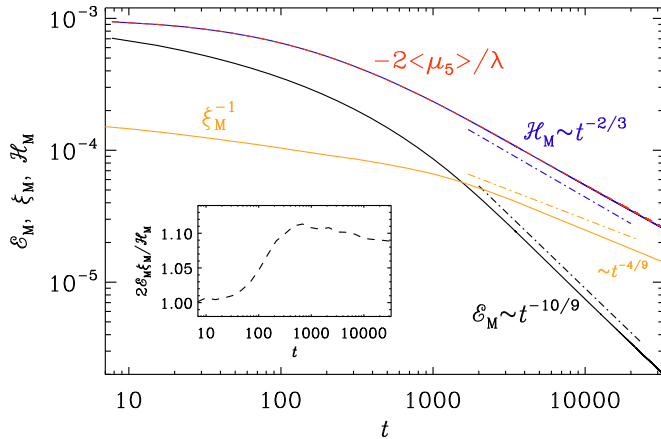


FIG. 3. Time dependence of \mathcal{E}_M (black), ξ_M (orange), \mathcal{H}_M (blue), and $-2\langle\mu_5\rangle/\lambda$ (red). The inset confirms that $2\mathcal{E}_M\xi_M/\mathcal{H}_M \approx 1$ during the whole time.

The approach to the point $(p, q) = (10/9, 4/9)$ does not occur predominantly along the $\beta = 3/2$ line, as in nonhelical standard MHD, but is now closer to the $r = 2/3$ line, where $p = q + r$. In the unbalanced case, where the net chirality is nonvanishing, however, the decay is solely governed by $\langle h_{\text{tot}} \rangle = \text{const}$ [37].

In conclusion, we have presented evidence that, in the balanced case of zero total chirality, the Hosking integral, when adapted to include the chiral chemical potential, is approximately conserved around the characteristic scale. This implies decay properties for magnetic energy and correlation length that are unchanged relative to nonhelical MHD, but here with $\mathcal{H}_M + 2\langle\mu_5\rangle/\lambda = 0$ (instead of $\mathcal{H}_M = 0$). This yields the scaling $|\mathcal{H}_M| \propto |\langle\mu_5\rangle| \propto t^{-2/3}$, along with the familiar scalings $\mathcal{E}_M \propto t^{-10/9}$ and $\xi_M \propto t^{4/9}$ that also apply to the case with $\mathcal{H}_M = 0$. These scalings have consequences for understanding the properties of the chiral magnetic effect in the early Universe [13, 18–20, 38] and young neutron stars [39, 40]. Our work has significant impact on the baryon asymmetry of the Universe from hypermagnetic helicity decay after axion

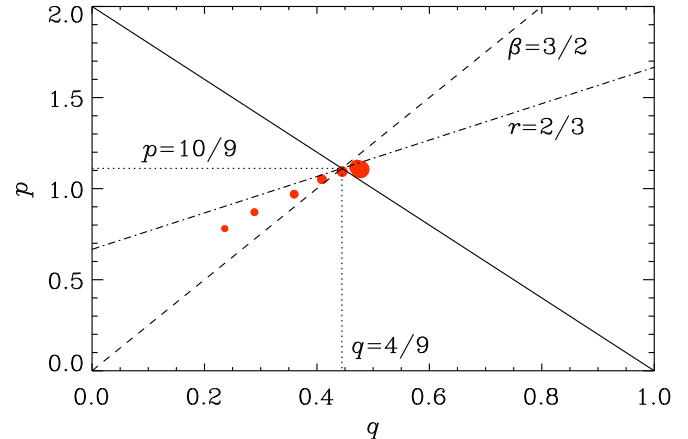


FIG. 4. pq diagram for times $t = 700, 1000, 1500, 2200, 3200, 4600, 6800, 10^4, 1.5 \times 10^4, 1.5 \times 10^4, 2.2 \times 10^4, 3.2 \times 10^4$, corresponding to symbols of increasing size. The solid line denotes the scale-invariance line $p = 2(1 - q)$, the dashed line the $\beta = 3/2$ line for adapted Hosking scaling, and the dashed dotted line is the new $r = 2/3$ line that does not have any correspondence in standard MHD.

inflation. It also exposes a rather unexpected application of the general idea behind the recently developed Hosking integral, raising therefore the hope that there may be other ones yet to be discovered.

We thank Valerie Domcke and Kai Schmitz for useful comments on the manuscript and Kyohei Mukaida for fruitful discussions. Support through Grant No. 2019-04234 from the Swedish Research Council (Vetenskapsrådet) (A.B.), Grant-in-Aid for Scientific Research No. (C) JP19K03842 from the JSPS KAKENHI (K.K.), and the Grant No. 185863 from the Swiss National Science Foundation (J.S.) are gratefully acknowledged. We acknowledge the allocation of computing resources provided by the Swedish National Infrastructure for Computing (SNIC) at the PDC Center for High Performance Computing Stockholm and Linköping.

- [1] L. Woltjer, A theorem on force-free magnetic fields, *Proc. Natl. Acad. Sci.* **44**, 489 (1958).
- [2] J. B. Taylor, Relaxation of Toroidal Plasma and Generation of Reverse Magnetic Fields, *Phys. Rev. Lett.* **33**, 1139 (1974).
- [3] A. Brandenburg and K. Subramanian, Astrophysical magnetic fields and nonlinear dynamo theory, *Phys. Rep.* **417**, 1 (2005).
- [4] D. N. Hosking and A. A. Schekochihin, Reconnection-Controlled Decay of Magnetohydrodynamic Turbulence and the Role of Invariants, *Phys. Rev. X* **11**, 041005 (2021).
- [5] A. A. Schekochihin, MHD turbulence: A biased review, *J. Plasma Phys.* **88**, 155880501 (2022).
- [6] H. Zhou, R. Sharma, and A. Brandenburg, Scaling of the Hosking integral in decaying magnetically dominated turbulence, *J. Plasma Phys.* **88**, 905880602 (2022).
- [7] A. Boyarsky, J. Fröhlich, and O. Ruchayskiy, Self-Consistent Evolution of Magnetic Fields and Chiral Asymmetry in the Early Universe, *Phys. Rev. Lett.* **108**, 031301 (2012).
- [8] I. Rogachevskii, O. Ruchayskiy, A. Boyarsky, J. Fröhlich, N. Kleeorin, A. Brandenburg, and J. Schober, Laminar and turbulent dynamos in chiral magnetohydrodynamics. I. Theory, *Astrophys. J.* **846**, 153 (2017).
- [9] S. L. Adler, Axial vector vertex in spinor electrodynamics, *Phys. Rev.* **177**, 2426 (1969).
- [10] J. S. Bell and R. Jackiw, A PCAC puzzle: $\pi^0 \rightarrow \gamma\gamma$ in the σ model, *Nuovo Cimento A* **60**, 47 (1969).
- [11] M. Joyce and M. Shaposhnikov, Primordial Magnetic Fields, Right Electrons, and the Abelian Anomaly, *Phys. Rev. Lett.* **79**, 1193 (1997).
- [12] Y. Akamatsu and N. Yamamoto, Chiral Plasma Instabilities, *Phys. Rev. Lett.* **111**, 052002 (2013).
- [13] K. Kamada, Return of grand unified theory baryogenesis: Source of helical hypermagnetic fields for the baryon asymmetry of the universe, *Phys. Rev. D* **97**, 103506 (2018).

- [14] V. Domcke, K. Kamada, K. Mukaida, K. Schmitz, and M. Yamada, A new constraint on primordial lepton flavour asymmetries, [arXiv:2208.03237](#).
- [15] R. T. Co, V. Domcke, and K. Harigaya, Baryogenesis from decaying magnetic helicity in axiogenesis, [arXiv:2211.12517](#).
- [16] Y. Hirono, D. E. Kharzeev, and Y. Yin, Self-similar inverse cascade of magnetic helicity driven by the chiral anomaly, *Phys. Rev. D* **92**, 125031 (2015).
- [17] J. Schober, T. Fujita, and R. Durrer, Generation of chiral asymmetry via helical magnetic fields, *Phys. Rev. D* **101**, 103028 (2020).
- [18] V. Domcke and K. Mukaida, Gauge field and fermion production during axion inflation, *J. Cosmol. Astropart. Phys.* **11** (2018) 020.
- [19] V. Domcke, B. von Harling, E. Morgante, and K. Mukaida, Baryogenesis from axion inflation, *J. Cosmol. Astropart. Phys.* **10** (2019) 032.
- [20] V. Domcke, K. Kamada, K. Mukaida, K. Schmitz, and M. Yamada, Wash-in leptogenesis after axion inflation, *J. High. Energy Phys.* **01** (2023) 053.
- [21] M. Giovannini and M. E. Shaposhnikov, Primordial hypermagnetic fields and triangle anomaly, *Phys. Rev. D* **57**, 2186 (1998).
- [22] M. Giovannini and M. E. Shaposhnikov, Primordial Magnetic Fields, Anomalous Matter-Antimatter Fluctuations, and Big Bang Nucleosynthesis, *Phys. Rev. Lett.* **80**, 22 (1998).
- [23] K. Kamada and A. J. Long, Evolution of the baryon asymmetry through the electroweak crossover in the presence of a helical magnetic field, *Phys. Rev. D* **94**, 123509 (2016).
- [24] K. Kamada, N. Yamamoto, and D.-L. Yang, Chiral effects in astrophysics and cosmology, *Prog. Part. Nucl. Phys.* **129**, 104016 (2023).
- [25] A. Brandenburg, J. Schober, I. Rogachevskii, T. Kahniashvili, A. Boyarsky, J. Fröhlich, O. Ruchayskiy, and N. Kleeorin, The turbulent chiral magnetic cascade in the early universe, *Astrophys. J.* **845**, L21 (2017).
- [26] A. Brandenburg, Y. He, T. Kahniashvili, M. Rheinhardt, and J. Schober, Relic gravitational waves from the chiral magnetic effect, *Astrophys. J.* **911**, 110 (2021).
- [27] A. Brandenburg, T. Kahniashvili, S. Mandal, A. R. Pol, A. G. Tevzadze, and T. Vachaspati, Evolution of hydromagnetic turbulence from the electroweak phase transition, *Phys. Rev. D* **96**, 123528 (2017).
- [28] R. Durrer and C. Caprini, Primordial magnetic fields and causality, *J. Cosmol. Astropart. Phys.* **11** (2003) 010.
- [29] Pencil Code Collaboration, A. Brandenburg, A. Johansen, P. Bourdin, W. Dobler, W. Lyra, M. Rheinhardt, S. Bingert, N. Haugen, A. Mee, F. Gent, N. Babkovskaia, C.-C. Yang, T. Heinemann, B. Dintrans, D. Mitra, S. Candelaresi, J. Warnecke, P. Käpylä, A. Schreiber *et al.*, The Pencil Code, a modular MPI code for partial differential equations and particles: Multipurpose and multiuser-maintained, *J. Open Source Softw.* **6**, 2807 (2021).
- [30] J. Schober, I. Rogachevskii, A. Brandenburg, A. Boyarsky, J. Fröhlich, O. Ruchayskiy, and N. Kleeorin, Laminar and turbulent dynamos in chiral magnetohydrodynamics. II. Simulations, *Astrophys. J.* **858**, 124 (2018).
- [31] J. Schober, A. Brandenburg, and I. Rogachevskii, Chiral fermion asymmetry in high-energy plasma simulations, *Geophys. Astrophys. Fluid Dyn.* **114**, 106 (2020).
- [32] A. Brandenburg, Hosking integral in nonhelical Hall cascade, *J. Plasma Phys.* **89**, 175890101 (2023).
- [33] A. Brandenburg and T. Kahniashvili, Classes of Hydrodynamic and Magnetohydrodynamic Turbulent Decay, *Phys. Rev. Lett.* **118**, 055102 (2017).
- [34] P. Olesen, Inverse cascades and primordial magnetic fields, *Phys. Lett. B* **398**, 321 (1997).
- [35] See also the discussion in Ref. [41] for weak magnetic field with zero magnetic helicity, where selfsimilarity is not assumed.
- [36] T. Kahniashvili, A. G. Tevzadze, A. Brandenburg, and A. Neronov, Evolution of primordial magnetic fields from phase transitions, *Phys. Rev. D* **87**, 083007 (2013).
- [37] A. Brandenburg, K. Kamada, K. Mukaida, K. Schmitz, and J. Schober, Chiral magnetohydrodynamics with zero total chirality, [arXiv:2304.06612](#).
- [38] L. Del Zanna and N. Bucciantini, Covariant and 3 + 1 equations for dynamo-chiral general relativistic magnetohydrodynamics, *Mon. Not. R. Astron. Soc.* **479**, 657 (2018).
- [39] Y. Masada, K. Kotake, T. Takiwaki, and N. Yamamoto, Chiral magnetohydrodynamic turbulence in core-collapse supernovae, *Phys. Rev. D* **98**, 083018 (2018).
- [40] M. Dvornikov, V. B. Semikoz, and D. D. Sokoloff, Generation of strong magnetic fields in a nascent neutron star accounting for the chiral magnetic effect, *Phys. Rev. D* **101**, 083009 (2020).
- [41] F. Uchida, M. Fujiwara, K. Kamada, and J. Yokoyama, New description of the scaling evolution of the cosmological magneto-hydrodynamic system, [arXiv:2212.14355](#).